Towards a sensitive search for variation of the fine-structure constant using radio-frequency $E1$ transitions in atomic dysprosium

A. T. Nguyen*
Department of Physics, University of California at Berkeley, Berkeley, California 94720-7300, USA

D. Budker†
Department of Physics, University of California at Berkeley, Berkeley, California 94720-7300, USA
and Nuclear Science Division, Lawrence Berkeley National Laboratory, Berkeley, California 94720, USA

S. K. Lamoreaux‡ and J. R. Torgerson§
University of California, Los Alamos National Laboratory, Physics Division, P-23, MS-H803, Los Alamos, New Mexico 87545, USA
(Received 28 August 2003; published 12 February 2004)

It has been proposed that the radio-frequency electric-dipole ($E1$) transition between two nearly degenerate opposite-parity states in atomic dysprosium should be highly sensitive to possible temporal variation of the fine-structure constant (α) [V. A. Dzuba, V. V. Flambaum, and J. K. Webb, Phys. Rev. A **59**, 230 (1999)]. We analyze here an experimental realization of the proposed search in progress in our laboratory, which involves monitoring the $E1$ transition frequency over a period of time using direct frequency counting techniques. We estimate that a statistical sensitivity of $|\dot{\alpha}/\alpha| \sim 10^{-18}$/yr may be achieved and discuss possible systematic effects that may limit such a measurement.

DOI: 10.1103/PhysRevA.69.022105 PACS number(s): 06.20.Jr, 32.30.Bv

I. INTRODUCTION

Variation of the fundamental constants of nature would signify new physics beyond the standard model, as discussed in a recent review [1]. Various theories constructed to unify gravity with the other forces allow or necessitate such a variation [2–5]. Of recent interest is the astrophysical evidence for a variation of the fine-structure constant α. From an analysis of quasar absorption spectra [6] over the redshift range $0.5<z<3.5$, a 4σ deviation of $\Delta\alpha/\alpha=(-0.72 \pm 0.18)\times 10^{-5}$ from zero was reported. Although these data hint at nonlinear dependence of α with time, for simplicity we assume a linear shift over $\sim 10^{10}$ yrs, which corresponds to a temporal variation of $\dot{\alpha}/\alpha=(7.2\pm 1.8)\times 10^{-16}$/yr. The current best terrestrial limit, over a much shorter time scale of 2 billion years, is $|\dot{\alpha}/\alpha|<10^{-18}$/yr [7–9], which comes from an analysis of geophysical data obtained from a natural fission reactor at Oklo (Gabon) which operated 1.8×10^9 yrs ago. Observational measurements like these, however, are subject to numerous assumptions which tend to complicate the interpretation. For example, questions have been recently raised regarding the reliability of the Oklo analysis [10].

Laboratory searches have numerous advantages, but have, thus far, placed weaker limits on $\dot{\alpha}$. For example, a comparison between H-maser and Hg^+ gave $\dot{\alpha}/\alpha \leqslant 3.7\times 10^{-14}$/yr [11], while a similar comparison between Rb and Cs microwave clocks yielded $|\dot{\alpha}/\alpha| \leqslant 1.6\times 10^{-15}$/yr [12]. A limit of $|\dot{\alpha}/\alpha|<1.2\times 10^{-15}$/yr was obtained from a comparison of a Hg^+ optical clock to a Cs microwave clock [13] using a frequency comb.

It has been suggested [14,15] that the electric-dipole ($E1$) transition between two nearly degenerate opposite-parity states in atomic dysprosium (Dy; $Z=66$) should be highly sensitive to variations in α. Indeed, a recent calculation [16] supports this conclusion. An experimental search utilizing these states is currently underway and is discussed here. We provide an analysis of possible systematic effects and show that this search could ultimately reach a sensitivity of $|\dot{\alpha}/\alpha| \sim 10^{-18}$/yr.

II. VARIATION OF α IN DYSPROSIUM

Tests of variation of α in atomic systems rely upon the fact that relativistic corrections depend differently on α for different energy levels. The total energy of a level can be written as

$$E=E_0+q(\alpha^2/\alpha_0^2-1)+O(\alpha^3), \tag{1}$$

where E_0 is the present-day energy, α_0 is the present-day value of the fine-structure constant, and q is a coefficient which determines the sensitivity to variations of α. This coefficient mainly depends upon the electronic configuration of the level. A recent calculation [16], utilizing relativistic Hartree-Fock and configuration interaction methods, found values of q for two nearly degenerate opposite-parity states in atomic dysprosium that are both large and of opposite sign. For the even-parity state (designated as A) $q_A/hc = 6008\ \mathrm{cm}^{-1}$, while for the odd-parity state (designated as

*Electronic address: atn@socrates.berkeley.edu
†Electronic address: budker@socrates.berkeley.edu
‡Electronic address: lamore@lanl.gov
§Electronic address: torgerson@lanl.gov

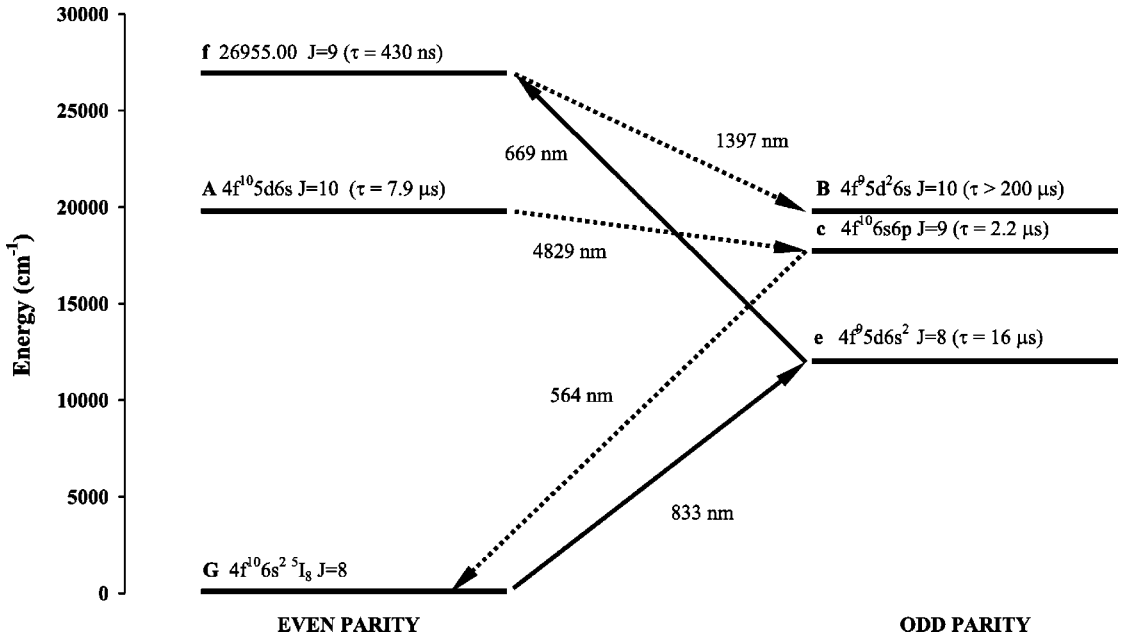

FIG. 1. Partial energy-level diagram of dysprosium showing the present scheme to populate level *B* and detect the population of level *A*. Solid lines, absorption. Dashed lines, spontaneous emission.

B) $q_B/hc=-23708$ cm^{-1}. The time variation of the transition frequency between levels *A* and *B* is (for $\alpha\approx\alpha_0$)

$$\dot{\nu}=2\frac{q_B-q_A}{h}\dot{\alpha}/\alpha\sim-2\times10^{15}\ \text{Hz}\ \ \dot{\alpha}/\alpha. \tag{2}$$

In other words, $|\dot{\alpha}/\alpha|=10^{-15}$/yr, implies $|\dot{\nu}|=2$ Hz/yr.

The statistical uncertainty of determining the central frequency from a resonance line shape is $\delta\nu\sim\gamma/\sqrt{N}$, where N is the number of counts and γ is the transition width. In the dysprosium system, $\gamma=20$ kHz is determined mainly by the lifetime of state *A*, $\tau_A=7.9$ μs ($\tau_B>200$ μs) [17]. A reasonable counting rate of 10^9 s^{-1} corresponds to a statistical sensitivity to ν_0 of $\sim0.6\ \tau^{-1/2}$ Hz$\sqrt{\text{s}}$, where τ is the integration time in seconds. After an integration time of 1 day, $\delta\nu\sim2$ mHz, thus allowing for a statistical sensitivity of $|\dot{\alpha}/\alpha|\sim10^{-18}$/yr for two measurements separated by a year's time.

It should be noted that the sensitivity to a variation in α is not proportional to $\delta\nu/\nu$. In fact, if ν is sufficiently small, the uncertainty in its determination is no longer limited by the relative uncertainty of the reference clock frequency (ν_{clock}), but rather by other experimental uncertainties. For example, a modest Cs clock provides an absolute accuracy of 10^{-12}. In the Dy transitions considered here, typical frequencies are ~1 GHz or smaller. Thus the clock uncertainty will only become an issue when other uncertainties can be reduced to the level of

$$\nu\frac{\delta\nu_{clock}}{\nu_{clock}}\sim10^{-3}\ \text{Hz}, \tag{3}$$

and even then can be overcome in a straightforward way by using a better reference clock.

The relatively modest requirement for the reference clock also means that the Dy experiment is insensitive to a variation of the clock's frequency due to a change in fundamental constants. For example, if α varies by 10^{-15}, the fractional change in the Cs clock frequency will be 2×10^{-15}, as the hyperfine transition frequency employed in the clock is proportional to α^2. This variation is negligible in comparison with the clock stability of 10^{-12}.

III. EXPERIMENTAL TECHNIQUE

A. Overview

The experimental search for a variation of the $E1$ transition frequency between the two opposite-parity states will proceed as follows. As shown in Fig. 1, atoms are populated [18] to the longer-lived odd-parity state *B* ($\tau_B>200$ μs [17]) via three transitions. The first two transitions require light at 833 nm and 669 nm, respectively. The third transition involves spontaneous decay with a branching ratio of 30% and the emission of 1397-nm light. Once in state *B*, atoms are transferred to state *A* with a rf electric field, whose frequency is referenced to a commercial Cs frequency standard. A resonance line shape is attained by scanning the rf frequency and monitoring 564-nm light from the second step of fluorescence from state *A*.

B. rf transitions

Because the energy separation between the nearly degenerate levels is on the order of hyperfine splittings and isotope shift energies (Fig. 2), and because dysprosium has seven stable isotopes, there are many choices of rf frequencies. Table I shows rf transitions with frequencies below 2 GHz calculated from measured hyperfine constants and isotope shifts [17]. The smallest transition frequency (3.1 MHz) oc-

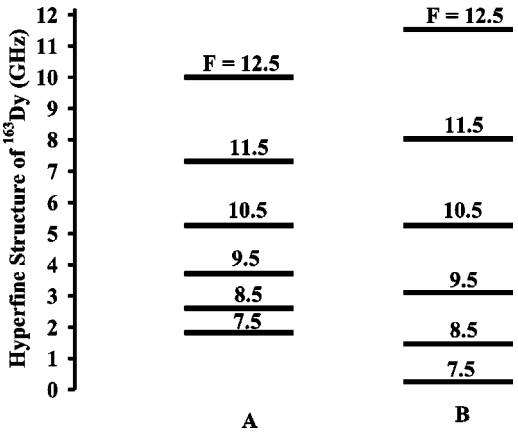

FIG. 2. Hyperfine structure of of *A* and *B* levels of ^{163}Dy. Zero energy is chosen for the lowest hyperfine component.

curs for the $F=10.5$ components of ^{163}Dy (the same transition is used in a search for parity nonconservation (PNC) [20]). A low-frequency transition that offers a higher counting rate is the 235 MHz transition in ^{162}Dy. This is due to a large isotopic abundance and the fact that there is no hyperfine splitting to dilute the atomic population. As discussed below, the choice of rf transition is also important in regard to sensitivity to systematic effects.

C. Apparatus

We have studied states *A* and *B* extensively as a system to measure atomic PNC effects [20]. Although our current apparatus is optimized for a PNC experiment, it is suitable for a measurement of $\dot{\alpha}$ with only minor modifications. We describe this system here in order to make a realistic evaluation of a possible experiment.

An atomic beam is produced by an effusive oven operating at 1500 K. The atoms pass through collimators and approach the interaction region (Fig. 3) where the desired electric and magnetic fields are produced. Inside the interaction region, the atoms encounter the laser beams used in the population scheme. The rf electric field is formed between two wire grids which are used in order to minimize surface area and thus stray charge accumulation. Typical applied electric-field amplitudes are ~ 5 V/cm. If necessary, a magnetic field of up to ~ 4 G can be applied parallel to the electric field. It is produced by eight turns of gold-plated copper wire surrounding the interaction region. The entire interaction region is placed inside a magnetic shield. As atoms decay from state *A*, 564-nm light from the second step of fluorescence (Fig. 1) is collected by a light pipe and detected by a photomultiplier tube. The extent of the light pipe area is shown by the dashed box in Fig. 3.

An example of a resonance line shape attained with this apparatus is shown in Fig. 4. Here, a magnetic field is scanned in the presence of a dc electric field revealing Zeeman-level-crossing resonances for ^{163}Dy. For the measurement of $\dot{\alpha}$, the signal to noise will be much greater as individual Zeeman resonances will not be resolved.

TABLE I. Calculated $E1$ transition frequencies using the hyperfine constants and isotope shifts from Ref. [17]. $||d_F||$ and $||d_J|| = 1.5(1)\times 10^{-2}$ $ea_0 \approx 19$ kHz/(V/cm) are reduced matrix elements. The last three columns list the isotope mass numbers (and abundances) and total angular momenta of the states involved in the transition.

ν_{rf} (MHz)	$\|\|d_F\|\|/\|\|d_J\|\|$	Mass No. (Abund.)	F_A	F_B
−1328.6	1.00	160 (2%)	10	10
−1856.4	0.15		7.5	8.5
−1714.7	1.04		11.5	11.5
−1249.7	0.99		10.5	10.5
−962.3	0.15		12.5	11.5
−791.5	0.94	161	9.5	9.5
−349.2	0.89	(19%)	8.5	8.5
−172.7	0.19		11.5	10.5
68.9	0.86		7.5	7.5
514.0	0.20		10.5	9.5
1096.9	0.19		9.5	8.5
1576.0	0.15		8.5	7.5
−234.7	1.00	162 (26%)	10	10
−1967.8	0.15		12.5	11.5
−1581.3	0.86		7.5	7.5
−1134.9	0.89		8.5	8.5
−609.7	0.94		9.5	9.5
−363.2	0.15	163	7.5	8.5
3.1	0.99	(25%)	10.5	10.5
504.6	0.19		8.5	9.5
713.1	1.04		11.5	11.5
1531.0	1.10		12.5	12.5
1543.9	0.20		9.5	10.5
753.5	1.00	164 (28%)	10	10

The interaction region can be improved by making it shorter, as most atoms decay within twice the lifetime of state *A* ($\tau_A = 7.9$ μs). Given a mean atomic velocity of 5×10^4 cm/s, an appropriate length will be ~ 8 mm. Furthermore, a shorter interaction region will allow for improved light collection efficiency, better suppression of background oven light, and better control over *E* and *B* fields.

D. Line shape

The natural line shape is a Lorentzian with a width ($\gamma \approx 20$ kHz) determined mainly by the lifetime of state A ($\tau_A = 7.9$ μs). To a first approximation, both transit time and

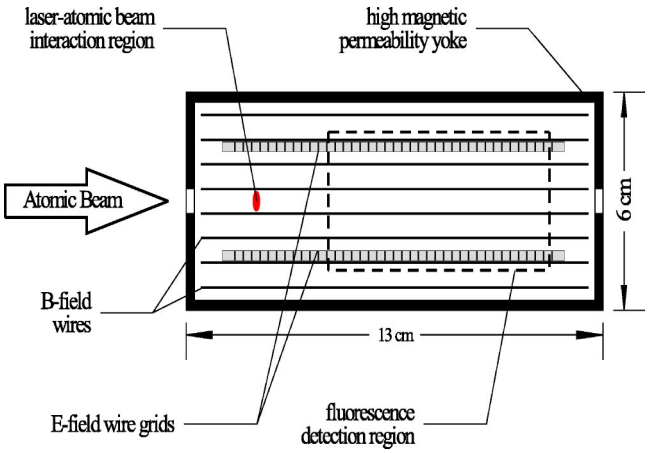

FIG. 3. Side view of interaction region currently optimized for PNC search.

Doppler broadening change the line shape in a symmetrical fashion. For an interaction length ~ 10 cm and a mean atomic velocity of $v=5\times10^4$ cm/s, the transit-time width is ~ 5 kHz. The Doppler shift (for an atom moving along the propagation direction of a free electromagnetic wave of frequency ν) goes as $\sim \nu(v/c)$, which for a 1 GHz transition is ~ 2 kHz. Thus, both transit-time and Doppler broadening contributions to the width are much smaller than the natural linewidth. Moreover, note that symmetrical broadening of the resonance does not change the central frequency. In addition, although an asymmetrical resonance can cause an apparent shift of the central frequency, this is not important for the search for variation of α as long as the asymmetry does not change between measurements.

In the following section, we discuss mechanisms leading to possible line shape asymmetry and estimate the corresponding shifts.

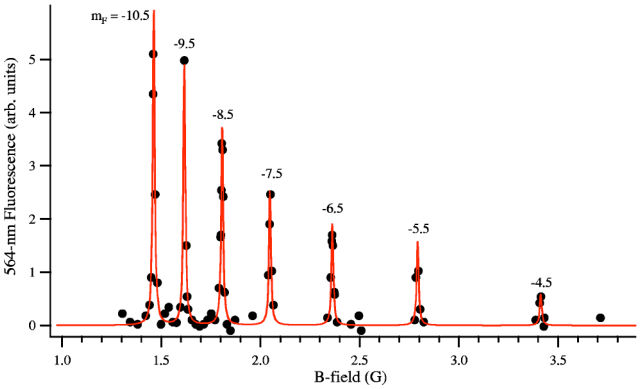

FIG. 4. Zeeman-level-crossing resonances for ^{163}Dy. State B is populated as shown in Fig. 1 in the presence of an electric field of 0.4 V/cm. The population of state A, resulting from electric-field-induced mixing of states A and B, is monitored by observing 564-nm fluorescence (Fig. 1). The solid line represents the best curve fit using the appropriate initial level separation [17] and g values [19].

TABLE II. Estimated sizes of systematic effects thus far considered.

Systematic shifts	Estimated size (Hz)
ac Stark[a]	$\sim(0.1-30)$
Doppler effect	<0.2
Room temp. black-body radiation	$\lesssim 0.1$
Oven black-body radiation	$\lesssim 0.02$
dc Stark[a]	$\sim(10^{-4}-10^{-2})$
collisional effects	$(1-10)\times10^{-4}$
Millman effect	$\lesssim 5\times10^{-4}$
Quadrupole moment	$\lesssim 10^{-5}$
Zeeman shift in stray B field	$\lesssim 10^{-5}$

[a]Transition dependent.

IV. SYSTEMATIC EFFECTS

High statistical sensitivity implies that our technique will likely be limited by how well we can control systematic effects. Below we analyze possible systematics and give estimates of how well various parameters of the experiment need to be controlled in order to achieve a sensitivity of $|\dot{\alpha}/\alpha|\sim10^{-18}$/yr. A summary of systematic effects and their estimated sizes is given in Table II.

A. dc Stark and quadrupole shifts

Variations of a stray dc electric field (E_{dc}) can give rise to time-varying frequency shifts for the transition frequency between states m and n,

$$\delta\nu_{dc}=\sum_{j\neq m}\frac{d_{mj}^2E_{dc}^2}{\Delta_{mj}}-\sum_{k\neq n}\frac{d_{nk}^2E_{dc}^2}{\Delta_{nk}}, \tag{4}$$

where d_{mj} and $\Delta_{mj}=E_m-E_j$ are the dipole matrix element and energy separation, respectively, between states m and j. The sum in Eq. (4) is taken over all states, including hyperfine levels in the case of an odd isotope.

The reduced dipole matrix element for the $B\rightarrow A$ transition is $||d_J||=1.5(1)\times10^{-2}$ ea$_0\approx19$ kHz/(V/cm) [17]. For large J, the maximum z projection of the dipole moment $\approx||d_J||/\sqrt{2J}=4$ kHz/(V/cm). Matrix elements connecting all levels with the same configurations as A and B have similar values [21]. Thus, between levels within 2000 cm^{-1} of the A and B levels, dipole matrix elements are relatively small, which reduces the sensitivity to systematics related to stray electric fields.

In an earlier PNC search, we reported stray dc E fields, presumably due to stray charge accumulation on the electrode surfaces, which varied on time scales from hours to months, and had a typical magnitude of 50 mV/cm [20]. Using this value for the field and $d\sim4$ kHz/(V/cm), we estimate the shift for transition frequencies in the range 3–1000 MHz to be $\sim10^{-4}$–10^{-2} Hz. The stray electric field can also be measured at a few mV/cm level using the atoms themselves [20] and canceled by the application of an external electric field.

An important systematic in Hg^+ optical clock experiments [22] is the electric quadrupole shift due to a stray-field gradient (∇E). Based upon the size of the interaction region and the homogeneity of the electric field for the Dy beam experiment (10^{-3}) [20], a conservative estimate gives $\nabla E \sim 10$ mV/cm^2. Assuming a typical a quadrupole moment $Q \sim 1\ ea_0^2$ leads to a quadrupole shift estimated to be $\lesssim 10^{-5}$ Hz which is negligible.

B. ac Stark shift

Fluctuations of the rf electric-field amplitude (E) can also lead to time-varying shifts. The second-order ac Stark shift for a two-level system is given by

$$\delta\nu_{ac} = \frac{d^2E^2}{2}\mathrm{Re}\left\{\frac{1}{\Delta-\nu+i\gamma}+\frac{1}{\Delta+\nu+i\gamma}\right\}, \tag{5}$$

where ν is the applied rf frequency, d is the dipole matrix element, and Δ is the energy separation. Because the first term is an odd function of detuning, only the second so-called Bloch-Siegert term contributes to an actual shift of the central frequency of the resonance line shape. For $\nu=\Delta \gg \gamma$ and a transition near saturation for which $d^2E^2/\gamma^2 \sim 1$, the corresponding shift is $\delta\nu_{ac} \sim \gamma^2/(4\Delta)$. Hence for $\gamma = 20$ kHz and transition frequencies ~ 3–1000 MHz, the shift varies from ~ 0.1 to 30 Hz. For the 3.1 MHz transition, for which the shift is largest, in order to achieve a sensitivity to frequency shifts of a few mHz, the amplitude stability must be better than 10^{-4}. However, this requirement becomes much less stringent for higher-frequency transitions. For $\nu \sim 1$ GHz, only a modest control at a level of a few percent is required.

We now consider frequency shifts due to all other levels on the transition frequency between levels m and n,

$$\delta\nu'_{ac} = \sum_{j\neq m,n}\frac{d_{mj}^2E^2}{4}\left(\frac{1}{\Delta_{mj}-\nu}+\frac{1}{\Delta_{mj}+\nu}\right) - \sum_{k\neq m,n}\frac{d_{nk}^2E^2}{4}\left(\frac{1}{\Delta_{nk}-\nu}+\frac{1}{\Delta_{nk}+\nu}\right), \tag{6}$$

where d_{mj} is the dipole matrix element and $\Delta_{mj}=E_m-E_j$ is the energy separation between levels m and j. The transition widths have been ignored because these levels are off resonant. For even isotopes, this shift is ~ 0.3 Hz and is mostly determined by levels which are >2000 cm^{-1} away with dipole matrix elements $\sim 1\ ea_0$. A comparable shift occurs for odd isotopes, assuming a particular choice of hyperfine transitions for which $\Delta_{mj}-\nu \sim 1$ GHz and $d_{mj} \sim 4$ kHz/(V/cm). Thus, taking into account the shifts due to other levels does not lead to more stringent requirements on the amplitude stability of the rf electric field beyond those obtained in the two-level approximation.

C. Stray magnetic fields

The residual magnetic field (B) can be controlled to $\sim 1\ \mu$G in the magnetically shielded interaction region. This corresponds to Zeeman shifts $g_F\mu_0 B \sim 1$ Hz, where μ_0 is the Bohr magneton and g_F is the Landé g factor (Table III). If the Zeeman sublevels are equally populated but still unresolved, then this field does not shift the central frequency of a resonance line shape but rather only broadens the line shape with a corresponding width of $\sim F(g_{FB}-g_{FA})\mu_0 B \approx 1$ Hz. However, an imbalance of sublevel populations can lead to asymmetric broadening of the resonance line shape, causing an apparent shift in the central frequency. In the experimental geometry discussed (Fig. 3), such an imbalance may be caused by residual circular polarization coupled with misalignments of the propagation direction of the linearly polarized light beams used in the first and second step of the population. Because residual circular polarization can be controlled to the level of $\sim 10^{-5}$ using standard polarimetric techniques, the shift of the resonance frequency can be made $\ll 10^{-5}$ Hz.

TABLE III. g values for the hyperfine levels of states A and B ($g_{JA}=1.21$ and $g_{JB}=1.367$ [19]).

F	g_{FA}	g_{FB}
7.5	1.57	1.77
8.5	1.36	1.54
9.5	1.22	1.38
10.5	1.11	1.26
11.5	1.03	1.16
12.5	0.968	1.09

D. Millman effect in electric resonance

Misalignments of the atomic beam and the geometry of the electrodes can cause the direction of the rf E field to rotate, as seen by a moving atom. This may lead to frequency shifts [23] analogous to the Millman effect encountered in magnetic resonance [24]. Let Ω be the frequency of this apparent E-field rotation. Because an oscillating field can be decomposed into two counter-rotating components, one of these components is shifted by $+\Omega$ and the other by $-\Omega$.

Using the measured homogeneity of our electric field, we estimate $\Omega \lesssim 50$ Hz. However, for a resonance line shape with unresolved sublevels, the central frequency remains largely unaffected. This is not true in the case of magnetic resonance (where transitions occur between magnetically split sublevels of the same level) and can be explained as follows: In the basis in which the quantization axis is perpendicular to the electric field, there are only σ_+ and σ_- transitions. The Millman effect causes shifts in the frequencies of these transitions as illustrated in Fig. 5 for a $\Delta J=0$ transition on resonance (where we have assumed that the

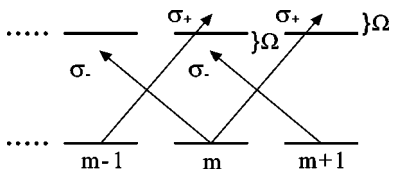

FIG. 5. Electric-field frequency shifts due to the Millman effect.

apparent electric-field rotation is in the same sense as the σ_+ component). If the sublevels of the initial state are equally populated and $\Omega \ll \gamma$, then these shifts only lead to a broadening of the line shape. However, if there is an imbalance of sublevel populations the broadening is asymmetric, which can cause an apparent shift in the central frequency by an amount $\sim \xi\Omega$, where ξ is the degree of atomic orientation. As mentioned earlier, residual circular polarization in the linearly polarized light, used in the first and second step of the population, may induce atomic orientation, but can be controlled to the level of $\sim 10^{-5}$, which is sufficient for the desired sensitivity to α. Furthermore, it should be noted that it is not the magnitude of the frequency shift but rather the stability that is important.

E. Black-body radiation

Black-body radiation (BBR) can cause ac Stark shifts [25]. The rms value of the black-body radiation electric field is

$$\langle E^2 \rangle = (8.3 \text{ V/cm})^2 [T(\text{K})/300 \text{ K}]^4. \tag{7}$$

A shift in the transition frequency arises from the difference in the ac Stark shifts experienced by levels *A* and *B*. We can give a rough estimate of this Stark shift ($\delta\nu_{BB}$) for one of these levels using Eq. (6),

$$\delta\nu_{BB} \sim \frac{d^2\langle E^2 \rangle}{4(\Delta - \nu_{BB})}, \tag{8}$$

where Δ is a characteristic atomic energy scale, ν_{BB} is a characteristic frequency of room-temperature BBR, and $d = 1 \text{ ea}_0$ is a typical optical transition dipole moment. Due to cancellations of contributions from nearby energy levels above and below the *A* and *B* levels, we assume that the net shift comes mainly from levels with large energy separations: $\nu_{BB} \ll \Delta \sim 10^{14}$ Hz, gives an estimate of $\delta\nu_{BB} \lesssim 0.1$ Hz.

The interaction region is illuminated by much hotter BBR from the atomic oven ($T \sim 1500$ K) which is ~ 15 cm away. However, the effect is smaller due to the decreased solid angle,

$$\begin{aligned} \delta\nu_{oven} &\sim \delta\nu_{BB} [T(\text{K})/300 \text{ K}]^4 \left(\frac{\Delta\Omega}{4\pi} \right), \\ &= 0.1 \text{ Hz} \left(\frac{1500 \text{ K}}{300 \text{ K}} \right)^4 \left(\frac{1 \text{ cm}^2}{4\pi 15^2 \text{ cm}^2} \right), \\ &= 0.02 \text{ Hz}, \end{aligned} \tag{9}$$

where we have assumed that an atom in the interaction region sees 1 cm^2 of hot surface.

The BBR shifts are large compared to the desired level of sensitivity and are difficult to eliminate. However, these shifts can be kept constant to the desired level by stabilizing the temperature of the interaction region (to $\sim 2\,^\circ$C) and the oven (to $\sim 30\,^\circ$C). For the oven, possible changes in surface emissivity will be a concern and requires further investigation.

F. Collisional shifts

Because the typical cross sections of the atomic collisions are on the order of 10^{-14} cm^2, most atoms in the atomic beam do not experience collisions with other atoms before they encounter the back wall of the interaction region. Collisional shifts of ~ 1–10 MHz/Torr (corresponding to the above-mentioned collisional cross-section values) are typically found for atomic transitions when the width is measured as a function of the atomic pressure. A possible effect of the rare collisions in the beam can be estimated by extrapolating these numbers to the low-pressure values corresponding to the beam environment. Assuming a 10 MHz/Torr shift due to collisions with residual gas, in order to keep time-dependent shifts below a few mHz, the residual gas pressure must be stable at a level $\sim 10^{-10}$ Torr. This can be achieved with standard ultrahigh-vacuum equipment. The pressure stability and composition of the residual gas will be monitored with a residual gas analyzer.

Note that we may find that collisional shifts are, in fact, much smaller than the above estimate because the *A*-*B* transition is nominally between *f* and *d* inner-shell electrons [26]. Another important effect that may reduce the effect of collisions on the measurement of the variation of α is that it is likely that an atom experiencing a collision will be quenched to a different atomic state, and, thus, will not produce a 564-nm fluorescent photon, and will therefore avoid detection.

A similar consideration applies to collisions between Dy atoms themselves. In the absence of collisional quenching, the worst-case estimate is that the present Dy density ($\sim 10^{10}$ atoms/cm^3) could give a shift of up to ~ 2 Hz. This effect will be investigated by measuring transition frequencies as a function of the atomic beam intensity and, if needed, the Dy beam intensity can be monitored and stabilized during measurement. Measuring a transition frequency at several different Dy-beam intensities will allow extrapolation to the collision-free value of the frequency. Technically, it is possible to vary the density of atomic in the atomic beam without significantly affecting other conditions of the experiment. For example, black-body radiation intensity in the interaction region can be maintained constant by separately controlling the front and back temperatures of the Dy oven. The BBR intensity is determined by the temperature of the front part of the oven near the nozzle, while the flux of atoms is determined by the lower temperature towards the back of the oven.

Another concern is a possible collisional wall-shift resulting from a fraction of the atoms reentering the interaction region upon reflection from its back wall. This effect is suppressed by a number of small factors: reflection probability, solid angle for entering the interaction region, the probability for an atom to avoid quenching in the wall collision, etc. If necessary, cryo cooling of the interaction-region walls may

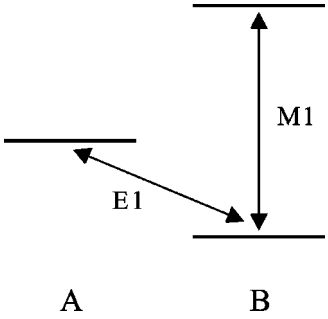

FIG. 6. Simultaneous measurement of an $M1$ transition frequency for a nonzero nuclear spin isotope facilitates the control of systematics.

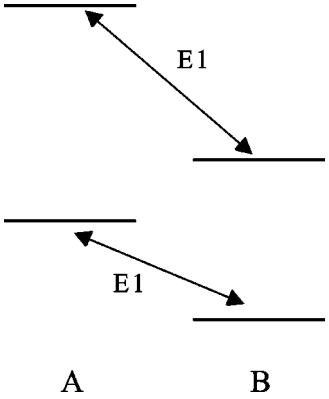

FIG. 7. Simultaneous measurement of two (or more) $E1$ transition frequencies to facilitate the control of systematics. This method works with the two zero-spin isotopes, ^{162}Dy and ^{164}Dy.

be employed to reduce the probability for an atom to bounce from it.

G. Doppler shift

The effect of the first-order Doppler shift is estimated to be small. To see this, we model the electric field (Fig. 3) as a standing wave constructed from two traveling waves counter-propagating colinearly with the direction of the atomic beam. Due to ohmic losses inside the conductors, the amplitude of each wave gets attenuated. A difference in the intensity of these waves at the location of the atoms leads to asymmetric Doppler broadening of the line shape, and thus an apparent shift. We estimate this intensity difference by first considering the B-field induced by the time-varying E field. This B-field penetrates inside the metal to within a skin depth, inducing currents from which the power loss can be readily calculated [27]. This simple model gives a fractional power difference $\propto \nu^{5/2}$. Since the Doppler shift for a given traveling-wave power is $\propto \nu$, the shift is $\propto \nu^{7/2}$. For a transition frequency of 1 GHz, we estimate the asymmetry to be $\lesssim 10^{-4}$ and the corresponding shift is ~ 0.2 Hz. One can imagine a factor of ~ 10 suppression if rf power is fed to the plates in a symmetric fashion. Thus, it is only required that this shift be stable to $\sim 10\%$ in order to achieve a sensitivity of a few mHz.

In addition to the first-order Doppler shift, we also consider the second-order effect. Depending upon the rf transition, the second-order Doppler shift is $\sim 10^{-3}$–10^{-6} Hz, which is sufficiently small.

H. Techniques to control systematics

A powerful method to detect and eliminate possible sources of systematic shifts common to both levels is to simultaneously measure the transition frequency between hyperfine levels of a given parity state. The reason is that, because the levels involved have the same relativistic corrections, this frequency is insensitive to variations of α. One possible scheme is to excite an $M1$ transition, e.g., as shown in Fig. 6, whose frequency can be monitored by looking for disappearance in the fluorescence from level A for a fixed $E1$ transition frequency. Alternatively, we can utilize another $E1$ transition as shown in Fig. 7. In this scenario, the effect α variation is twice as large in the sum of the two frequencies, while the difference is insensitive to α variations.

Furthermore, one can compare $E1$ transitions for the two abundant isotopes with zero nuclear spin (^{162}Dy and ^{164}Dy). The counting rate is significantly higher and the level structure is much simpler without hyperfine interactions.

V. DISCUSSION

In summary, rf $E1$ transitions in Dy provide an attractive system in which to test the temporal variation of α. The frequencies of these transitions can be directly counted. For a limit of $\dot{\alpha}/\alpha < 10^{-15}$/yr, the shift was calculated to be ≈ 2 Hz/yr. At present, a statistical sensitivity of 0.6 Hz in one second of integration time is achievable. Knowledge of systematic effects is critical to this experiment. Preliminary analysis shows that it may be possible to control them at a level corresponding to $|\dot{\alpha}/\alpha| \sim 10^{-18}$/yr, a level of sensitivity that would rival that of the most stringent observational limit set by the Oklo natural reactor.

ACKNOWLEDGMENTS

We thank D. F. Kimball, M. G. Kozlov, J. E. Stalnaker, and V. V. Yashchuk for valuable discussions. This work was supported in part by the UC Berkeley-LANL CLE program and a NIST Precision Measurement Grant. D.B. also acknowledges the support of the Miller Institute for Basic Research in Science.

[1] J. Uzan, Rev. Mod. Phys. **75**, 403 (2003).
[2] W.J. Marciano, Phys. Rev. Lett. **52**, 489 (1984).
[3] J.D. Barrow, Phys. Rev. D **35**, 1805 (1987).
[4] T. Damour and A.M. Polyakov, Nucl. Phys. **B423**, 532 (1994).
[5] T. Damour, F. Piazza, and G. Veneziano, Phys. Rev. Lett. **89**, 081601 (2002).

[6] J.K. Webb *et al.*, Phys. Rev. Lett. **87**, 091301 (2001).
[7] A.I. Shlyakhter, Nature (London) **264**, 340 (1976).
[8] T. Damour and F. Dyson, Nucl. Phys. **B480**, 37 (1996).
[9] Y. Fujii *et al.*, Nucl. Phys. **B573**, 377 (2000).
[10] S.K. Lamoreaux, e-print physics/0309048 at http://arxiv.org/
[11] J.D. Prestage, R.L. Tjoelker, and L. Maleki, Phys. Rev. Lett. **74**, 3511 (1995).
[12] H. Marion *et al.*, Phys. Rev. Lett. **90**, 150801 (2003).
[13] S. Bize *et al.*, Phys. Rev. Lett. **90**, 150802 (2003).
[14] V.A. Dzuba, V.V. Flambaum, and J.K. Webb, Phys. Rev. Lett. **82**, 888 (1999).
[15] V.A. Dzuba, V.V. Flambaum, and J.K. Webb, Phys. Rev. A **59**, 230 (1999).
[16] V.A. Dzuba, V.V. Flambaum, and M.V. Marchenko, Phys. Rev. A **68**, 022506 (2003).
[17] D. Budker, D. DeMille, E.D. Commins, and M.S. Zolotorev, Phys. Rev. A **50**, 132 (1994).
[18] A.T. Nguyen, G.D. Chern, D. Budker, and M. Zolotorev, Phys. Rev. A **63**, 013406 (2000).
[19] W.C. Martin, R. Zalubas, and L. Hagan, *Atomic Energy Levels-The Rare Earth Elements* (National Bureau of Standards, Washington, DC, 1978).
[20] A.T. Nguyen, D. Budker, D. DeMille, and M. Zolotorev, Phys. Rev. A **56**, 3453 (1997).
[21] V.A. Dzuba (private communication).
[22] W. Itano, J. Res. Natl. Inst. Stand. Technol. **105**, 829 (2000).
[23] L. Grabner and V. Hughes, Phys. Rev. **70**, 819 (1950).
[24] S. Millman, Phys. Rev. **55**, 628 (1939).
[25] V.G. Pal'chikov, Y.S. Domnin, and A.V. Novoselov, J. Opt. B: Quantum Semiclassical Opt. **5**, S131 (2003).
[26] V.D. Vedenin and V.N. Kulyasov, Opt. Spectrosc. **59**, 603 (1985).
[27] J.D. Jackson, *Classical Electrodynamics*, 2nd ed. (Wiley, New York, 1975).